

This is a repository copy of *Scalar radiation from a radially infalling source into a Schwarzschild black hole in the framework of quantum field theory*.

White Rose Research Online URL for this paper:  
<http://eprints.whiterose.ac.uk/126928/>

Version: Accepted Version

---

**Article:**

Oliveira, Leandro A., Crispino, Luis C. B. and Higuchi, Atsushi  
[orcid.org/0000-0002-3703-7021](https://orcid.org/0000-0002-3703-7021) (2018) Scalar radiation from a radially infalling source into a Schwarzschild black hole in the framework of quantum field theory. *European Physical Journal C (Particles and Fields)*. pp. 1-11. ISSN 1434-6052

<https://doi.org/10.1140/epjc/s10052-018-5604-8>

---

**Reuse**

Items deposited in White Rose Research Online are protected by copyright, with all rights reserved unless indicated otherwise. They may be downloaded and/or printed for private study, or other acts as permitted by national copyright laws. The publisher or other rights holders may allow further reproduction and re-use of the full text version. This is indicated by the licence information on the White Rose Research Online record for the item.

**Takedown**

If you consider content in White Rose Research Online to be in breach of UK law, please notify us by emailing [eprints@whiterose.ac.uk](mailto:eprints@whiterose.ac.uk) including the URL of the record and the reason for the withdrawal request.

# Scalar radiation from a radially infalling source into a Schwarzschild black hole in the framework of quantum field theory

Leandro A. Oliveira<sup>a,1,2</sup>, Luís C. B. Crispino<sup>b,2</sup>, Atsushi Higuchi<sup>c,3</sup>

<sup>1</sup>Campus Salinópolis, Universidade Federal do Pará, 68721-000, Salinópolis, Pará, Brazil

<sup>2</sup>Faculdade de Física, Universidade Federal do Pará, 66075-110, Belém, Pará, Brazil

<sup>3</sup>Department of Mathematics, University of York, YO10 5DD Heslington, York, United Kingdom

Received: date / Accepted: date

**Abstract** We investigate the radiation to infinity of massless scalar field from a source falling radially towards a Schwarzschild black hole using the framework of quantum field theory at tree level. In the case where the source falls from infinity, the monopole radiation is dominant for low initial velocities but higher multipoles become dominant at high initial velocities. It is found that, as in the electromagnetic and gravitational cases, at high initial velocities the energy spectrum for each multipole with  $l \geq 1$  is approximately constant up to the fundamental quasinormal frequency and then drops to zero. We also investigate the case where the source falls from rest at a finite distance from the black hole. We find that the monopole and dipole contributions are dominant in this case. We point out that this case needs to be distinguished carefully from the unphysical process where the source abruptly appears at rest and starts falling, which would result in radiation of an infinite amount of energy. We also investigate the radiation of massless scalar field to the horizon of the black hole, finding some features similar to the gravitational case.

## 1 Introduction

Black holes (BHs) stand out as the most relevant and simple objects described by General Relativity. BHs are trapped regions even to light, due to their extremely intense gravitational field. The boundary of no return, from which light cannot escape, the BH event horizon, is determined as a function of only three parameters associated to the BH, i.e. mass, angular momentum and electric charge [1]. Particles falling into BHs emit radiation which carries information to infinity about the event horizon, as a “fingerprint” of the

BHs [2–5]. Thus, in principle, evidence for the existence of an event horizon, and therefore for the existence of BHs, can be obtained by analyzing the radiation emitted from a source falling into BHs. The scientific literature about the dynamics of a test particle falling into BHs has developed significantly in the early 1970’s. The existing results for the problem of radiation emission from a particle falling radially into BHs were obtained using the formalism of Classical Field Theory (CFT) [2–17], and the investigation of this kind of problems from the viewpoint of Quantum Field Theory (QFT) has not been carried out. The formalism of QFT applied to the problem of radiation emission has been used for the determination of the radiation emission by sources and charges rotating around a BH, known as synchrotron radiation [18–25]. Furthermore, QFT has been used to investigate radiation emission from a uniformly accelerated source in flat spacetimes [26, 27] and also to investigate the interaction of sources with Hawking radiation [28–34]. In this paper, using QFT at tree level, we investigate in details the properties of the radiation emission due to the radial infall of a particle source of massless scalar field into a Schwarzschild BH. One of the main advantages in computing the emitted energy using the framework of QFT at level tree is that this approach makes the extension to the radiative quantum corrections more straightforward. We note in passing that the change in the geometry due to the Hawking radiation for an astrophysical black hole is extremely small [35] and, as a result, that it is legitimate to use the eternal black hole in our calculations.

The remainder of this paper is organized as follows. In Sec. 2 we briefly review the general formalism used in this paper. In Sec. 3 we describe the radial infall of a source into a Schwarzschild BH according to General Relativity. In Sec. 4 we obtain expressions for the emitted energy spectrum and the total emitted energy for a quantum scalar field minimally coupled to the scalar source. In Sec. 5 we ob-

<sup>a</sup>e-mail: laoliveira@ufpa.br

<sup>b</sup>e-mail: crispino@ufpa.br

<sup>c</sup>e-mail: atsushi.higuchi@york.ac.uk

tain the zero-frequency limit of the emitted energy spectra, using approximate analytic solutions. In Sec. 6 we analyze and discuss our numerical results for the radiation emission obtained from the viewpoint of QFT. We summarize some features of our results in Sec. 7. We use, unless otherwise stated, natural units with  $G = c = \hbar = 1$ .

## 2 General Formalism of QFT in Schwarzschild spacetime

The total Lagrangian density with a classical source  $j(x^\mu)$ , minimally coupled to a massless and chargeless scalar field  $\hat{\Phi}(x^\mu)$ , can be written as

$$\mathcal{L} = \sqrt{-g} \left( \frac{1}{2} \nabla^\mu \hat{\Phi} \nabla_\mu \hat{\Phi} + j \hat{\Phi} \right), \quad (1)$$

where  $g \equiv \det(g_{\mu\nu})$  is the determinant of the metric  $g_{\mu\nu}$ .

The line element  $ds^2 = g_{\mu\nu} dx^\mu dx^\nu$  of the Schwarzschild spacetime can be written as

$$ds^2 = f dt^2 - f^{-1} dr^2 - r^2 (d\theta^2 + \sin^2 \theta d\phi^2), \quad (2)$$

where  $f(r) = 1 - 2M/r$ . Note that  $f(r = r_h) = 0$ , with  $r_h \equiv 2M$  being the position of the event horizon of the Schwarzschild BH, and  $f(r \rightarrow \infty) = 1$ . This spacetime is asymptotically flat.

The scalar field  $\hat{\Phi}(x^\mu)$  can be expanded in terms of a complete set of positive- and negative-frequency modes,  $u_{\omega l m}$  and  $u_{\omega l m}^*$ , as

$$\hat{\Phi} = \sum_{l=0}^{\infty} \sum_{m=-l}^{m=l} \int_0^{\infty} d\omega \left[ u_{\omega l m} \hat{a}_{\omega l m} + u_{\omega l m}^* \hat{a}_{\omega l m}^\dagger \right], \quad (3)$$

with  $\omega > 0$ , where “\*” denotes complex conjugation, and  $\hat{a}_{\omega l m}$  and its Hermitian adjoint  $\hat{a}_{\omega l m}^\dagger$  are, respectively, the annihilation and the creation operators [36]. These operators satisfy the following non-vanishing commutation relations:

$$\left[ \hat{a}_{\omega l m}, \hat{a}_{\omega' l' m'}^\dagger \right] = \delta(\omega - \omega') \delta_{l l'} \delta_{m m'}. \quad (4)$$

Since the Schwarzschild spacetime is spherically symmetric, the positive-frequency modes  $u_{\omega l m}(x^\mu)$ , can be written as:

$$u_{\omega l m}(x^\mu) = C_{\omega l m} \frac{\Psi_{\omega l}^*(r)}{r} Y_{lm}(\theta, \phi) \exp(-i\omega t), \quad (5)$$

which satisfy the Klein-Gordon equation

$$\nabla_\mu \nabla^\mu u_{\omega l m} = \frac{1}{\sqrt{-g}} \partial_\mu (\sqrt{-g} g^{\mu\nu} \partial_\nu u_{\omega l m}) = 0, \quad (6)$$

where  $C_{\omega l m}$  is a normalization constant,  $Y_{lm}(\theta, \phi)$  are the spherical harmonics [37] and  $\sqrt{-g} = r^2 \sin \theta$  [obtained from the line element (2)]. The Klein-Gordon inner product for the mode functions is defined as follows:

$$\sigma_{KG}(\varphi_1, \varphi_2) = i \int_S dS^\mu \left[ \varphi_1^* \nabla_\mu \varphi_2 - (\nabla_\mu \varphi_2^*) \varphi_1 \right], \quad (7)$$

with  $dS^\mu = r^2 \sin \theta dr d\theta d\phi \delta_0^\mu / f(r)$ , where  $S$  is a constant-time hypersurface, which is a Cauchy surface [38]. The commutation relations (4) imply that the modes  $u_{\omega l m}$  are normalized as follows:

$$\sigma_{KG}(u_{\omega l m}, u_{\omega' l' m'}) = \delta(\omega - \omega') \delta_{l l'} \delta_{m m'}, \quad (8)$$

$$\sigma_{KG}(u_{\omega l m}^*, u_{\omega' l' m'}) = 0. \quad (9)$$

The conditions (8) determine the normalization constant  $C_{\omega l m}$  in Eq. (5).

Substituting Eq. (5) into the Klein-Gordon equation (6), we obtain the following ordinary differential equation for  $\Psi_{\omega l}(x)$ :

$$\left[ \frac{d^2}{dr_*^2} + \omega^2 - V_l(r) \right] \Psi_{\omega l}(r_*) = 0, \quad (10)$$

where  $V_l(r)$  is the effective potential, given by

$$V_l(r) = f(r) \left[ \frac{l(l+1)}{r^2} + \frac{1}{r} \frac{df}{dr} \right], \quad (11)$$

and the Regge-Wheeler coordinate  $r_*$  is defined by  $dr_*/dr \equiv f(r)^{-1}$ , which for the Schwarzschild BH can be explicitly written as

$$r_* = r + r_h \log(r/r_h - 1). \quad (12)$$

Equation (10) admits two independent sets of solutions, which can be represented by the modes  $\Psi_{\omega l}^{\text{up}}(r_*)$ , purely incoming from the past horizon  $H^-$ , and the modes  $\Psi_{\omega l}^{\text{in}}(r_*)$ , purely incoming from the past null infinity  $\mathcal{I}^-$ . The solutions  $\Psi_{\omega l}^{\text{up}}(r_*)$  and  $\Psi_{\omega l}^{\text{in}}(r_*)$  satisfy, respectively, the following boundary conditions at the event horizon ( $r_* \rightarrow -\infty$ ) and at spatial infinity ( $r_* \rightarrow \infty$ ):

$$\Psi_{\omega l}^{\text{up}}(r_*) \approx \begin{cases} A_{\omega l}^{\text{up}} \chi_{\text{hor}}^* + B_{\omega l}^{\text{up}} \chi_{\text{hor}} & (r_* \rightarrow -\infty), \\ \chi_{\text{inf}} & (r_* \rightarrow \infty), \end{cases} \quad (13)$$

and

$$\Psi_{\omega l}^{\text{in}}(r_*) \approx \begin{cases} \chi_{\text{hor}} & (r_* \rightarrow -\infty), \\ A_{\omega l}^{\text{in}} \chi_{\text{inf}}^* + B_{\omega l}^{\text{in}} \chi_{\text{inf}} & (r_* \rightarrow \infty). \end{cases} \quad (14)$$

The functions  $\chi_{\text{hor}}$  and  $\chi_{\text{inf}}$  are defined to be of the form  $\exp(-i\omega r_*)$  and  $\exp(i\omega r_*)$ , respectively, at leading order in  $1/r_*$ . In our numerical computations we write these functions near the horizon and near spatial infinity as

$$\chi_{\text{hor}} = \exp(-i\omega r_*) \sum_{j=0}^{j_{\text{max}}} a_j (r - r_h)^j, \quad (15)$$

$$\chi_{\text{inf}} = \exp(i\omega r_*) \sum_{j=0}^{j_{\text{max}}} \frac{b_j}{r^j}, \quad (16)$$

where the coefficients  $a_j$  and  $b_j$  are obtained from Eq. (10), with the choice  $a_0 = 1$  and  $b_0 = 1$ . We let  $j_{\text{max}} = 10$  in our

computation. The coefficients  $A_{\omega l}^{\text{up/in}}$  and  $B_{\omega l}^{\text{up/in}}$  are determined by matching the boundary conditions (13) and (14) with the numerical solution  $\psi_{\omega l}(r_*)$ , obtained from Eq. (10), at the event horizon  $r_* \rightarrow -\infty$  and at spatial infinity  $r_* \rightarrow \infty$ , respectively. Note that the coefficients  $A_{\omega l}^{\text{up/in}}$  and  $B_{\omega l}^{\text{up/in}}$  are related to the transmission coefficient  $|\mathcal{T}_{\omega l}^{\text{up/in}}|^2$  and reflection coefficient  $|\mathcal{R}_{\omega l}^{\text{up/in}}|^2$ , respectively, as follows:

$$|\mathcal{T}_{\omega l}^{\text{up/in}}|^2 \equiv \frac{1}{|A_{\omega l}^{\text{up/in}}|^2}, \quad (17)$$

and

$$|\mathcal{R}_{\omega l}^{\text{up/in}}|^2 \equiv \left| \frac{B_{\omega l}^{\text{up/in}}}{A_{\omega l}^{\text{up/in}}} \right|^2. \quad (18)$$

The reflection and transmission coefficients satisfy the following relation:

$$|\mathcal{R}_{\omega l}^{\text{up/in}}|^2 + |\mathcal{T}_{\omega l}^{\text{up/in}}|^2 = 1. \quad (19)$$

From the boundary conditions (13) and (14) and Eq. (8), we find that the normalization constant  $C_{\omega l m}$  can be written as

$$C_{\omega l m}^{\text{up/in}} = \frac{1}{\sqrt{4\pi\omega} A_{\omega l}^{\text{up/in}}}. \quad (20)$$

We note that, because of the complex conjugation in Eq. (5) of  $\psi_{\omega l}(r)$ , the modes  $u_{\omega l m}(x^\mu)$  are the modes purely ingoing into the future horizon  $H^+$  [with  $\psi_{\omega l}^{\text{up}*}(r)$ ] or purely outgoing to the future null infinity  $\mathcal{I}^+$  [with  $\psi_{\omega l}^{\text{in}*}(r)$ ]. These are the modes we use for computing the radiation into the horizon and to null infinity in the next section.

### 3 Radial infall of a source into a Schwarzschild Black Hole

We consider a source falling radially into a Schwarzschild BH. The source has zero angular momentum as a result. Without loss of generality we let the source fall along the  $z$ -axis. The stress-energy tensor for a point source can be written as

$$T^{\mu\nu} = \int \frac{d\tau}{\sqrt{-g}} q \delta^4[x^\alpha - x^\alpha(\tau)] \frac{dx^\mu}{d\tau} \frac{dx^\nu}{d\tau}, \quad (21)$$

where  $\tau$  is the source's proper time.

By setting  $j(x^\mu) = T_{\nu}^{\nu}$  (corresponding to a scalar source), we find the following expression for a massive source

$$j(x^\mu) = \frac{q}{\sqrt{-g} v^t} \delta(r - r_s) \delta(\theta - \theta_s) \delta(\phi - \phi_s), \quad (22)$$

where  $(r, \theta, \phi) = (r_s, \theta_s, \phi_s)$  refers to the spatial coordinates of the source at given time  $t$  in spherical polar coordinates,  $q$  is a coupling constant between the source and a massless and chargeless scalar field  $\hat{\Phi}$  [18, 32], and  $v^t$  is the contravariant  $t$ -component of the 4-velocity of the source. The factor  $1/v^t$  makes the source boost invariant along its trajectory.

The 4-velocity  $v^\mu$  of a source infalling radially is given by the following expression

$$v^\mu \equiv \frac{dx^\mu}{d\tau} = \left[ \frac{E}{f(r)}, -\sqrt{E^2 - f(r)}, 0, 0 \right], \quad (23)$$

where  $E$  is the source's conserved energy divided by its rest mass [1]. If the source has initial position  $r = r_0$  and velocity  $v_0$  in the ingoing radial direction (at  $t = 0$ ), then [38]

$$E = \sqrt{\frac{f(r_0)}{1 - [v_0/f(r_0)]^2}}. \quad (24)$$

Using Eqs. (2) and (23), we can find an expression for the modulus of the velocity of the source (falling radially) at position  $r$  in the static frame [39], namely

$$U_r = \left| f(r)^{-1} \frac{dr}{dt} \right| = \frac{1}{E} \sqrt{E^2 - f(r)}. \quad (25)$$

In Fig. 1, we exhibit plots of  $U_r$  for selected values of  $v_0$  and  $r_0$ .

We write the radial coordinate of the source as  $r_s \equiv r_s(t_s)$ , with  $t_s$  being the time coordinate in Eq. (2) associated with the trajectory of the radial infall along its geodesic. The function  $t_s(r_s)$  is obtained from the relation

$$\frac{dt_s}{dr_s} = -\frac{E}{f(r_s)\sqrt{E^2 - f(r_s)}}. \quad (26)$$

This formula follows from Eq. (23). Using the properties of the Dirac delta function and Eqs. (23) and (26), we can rewrite Eq. (22) as follows:

$$j(x^\mu) = \frac{q \delta(t - t_s) \delta(\theta - \theta_s) \delta(\phi - \phi_s)}{r_s^2 \sin \theta \sqrt{E^2 - f(r_s)}}, \quad (27)$$

where  $t_s(r)$  is the inverse function of  $r = r_s(t_s)$ . The constants  $\theta_s$  will be set to 0 (and then  $\phi_s$  will be ambiguous and can be set to any value).

### 4 Total Emitted Energy

Now we turn to the computation of the total emitted energy (for each multipole number  $l$  and azimuthal number  $m$ ) by a source  $j(x^\mu)$  minimally coupled to a scalar field  $\hat{\Phi}(x^\mu)$  in a background of a spherically symmetric spacetime using QFT at tree level. We start from the following expression [18, 19]:

$$E_{lm}^{\text{hor/inf}} = \int_0^\infty d\omega \omega |\mathcal{A}_{\omega l m}^{\text{up/in}}|^2, \quad (28)$$

where the labels ‘‘inf’’ and ‘‘hor’’ correspond to the energy radiated, respectively, to infinity and to the event horizon,

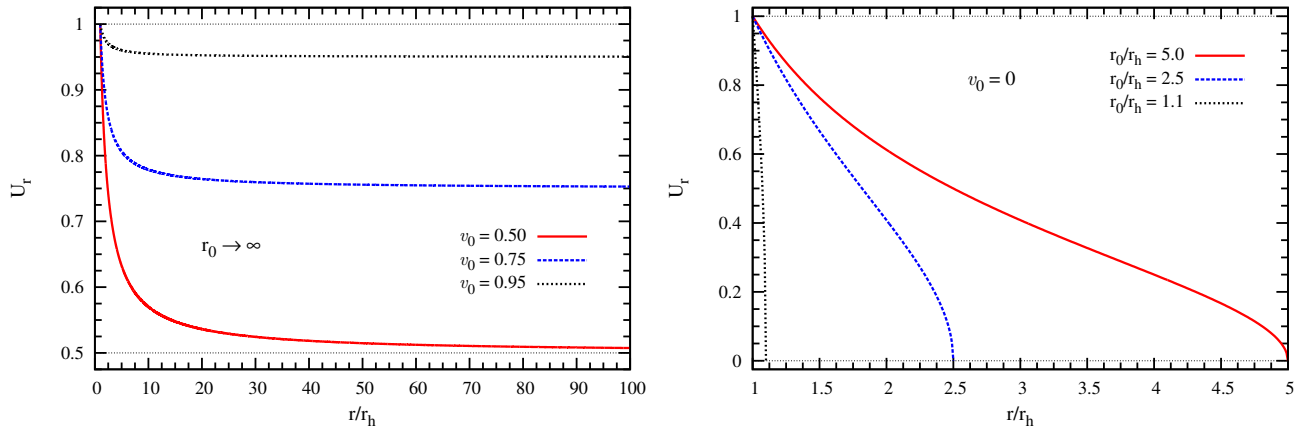


**Fig. 1** Modulus of the radial component of the velocity of the source (measured by a static observer, located at  $r$ , as particle passes by her [39]), as a function of  $r$ , for a source released from spatial infinity ( $r_0 \rightarrow \infty$ ) with initial velocity  $v_0 = 0.5$ ,  $v_0 = 0.75$  and  $v_0 = 0.95$  (plots on the left), and for a source infalling from rest ( $v_0 = 0$ ) released at positions  $r_0 = 5 r_h$ ,  $r_0 = 2.5 r_h$  and  $r_0 = 1.1 r_h$  (plots on the right).

and  $\mathcal{A}_{\omega l m}^{\text{up/in}}$  are the emission amplitudes at tree level given by

$$\mathcal{A}_{\omega l m}^{\text{up/in}} = \langle \omega l m | i \int d^4 x \sqrt{-g} j(x^\mu) \hat{\Phi}(x^\mu) | 0 \rangle, \quad (29)$$

corresponding to a transition between the vacuum state and one scalar particle state. By recalling that

$$\hat{a}_{\omega l m} | 0 \rangle = 0, \quad (30)$$

with  $| 0 \rangle$  being the Boulware vacuum [36, 40], and  $| \omega l m \rangle = \hat{a}_{\omega l m}^\dagger | 0 \rangle$ , we have, using the commutation relations (4),

$$\langle \omega l m | \hat{a}_{\omega' l' m'}^\dagger | 0 \rangle = \delta(\omega - \omega') \delta_{ll'} \delta_{mm'}. \quad (31)$$

Then, substituting Eq. (3) into Eq. (29), and using Eqs. (30) and (31), we find

$$\mathcal{A}_{\omega l m}^{\text{up/in}} = i \int d^4 x \sqrt{-g} j(x^\mu) u_{\omega l m}^*(x^\mu). \quad (32)$$

If we had chosen the Unruh or Hartle-Hawking vacuum [41, 42], then there would be absorption and stimulated emission of the scalar particles. The rates of these two processes would be exactly the same, and, as a result, the net emission would be the same as in the Boulware vacuum (see, e.g. [18, 43]). It is known that the Boulware vacuum is unphysical because the expectation value of the stress-energy tensor is singular at the past and future horizons for this state [44]. Our results can be regarded to be about the net emission from the scalar source in the Unruh vacuum, which is more physical.

As we stated before, we let the motion be along of the  $z$ -axis without loss of generality because of the spherical symmetry of Schwarzschild spacetime. Thus, we consider  $\theta_s = 0$  and  $\phi_s = 0$ . (The value of  $\phi_s$  is arbitrary once we have  $\theta_s = 0$ , but we choose this value for definiteness.) As a consequence, only the mode  $m = 0$  contributes to the emission

amplitude [9, 17]. Because of this fact, the only spherical harmonics which will be associated to non-vanishing amplitudes are  $Y_{l0}(\theta, \phi)$  with

$$Y_{l0}(0, 0) = \sqrt{\frac{2l+1}{4\pi}}. \quad (33)$$

From now on we will omit the azimuthal quantum number  $m$  from  $\mathcal{A}_{\omega l m}^{\text{up/in}}$  and  $E_{l m}^{\text{hor/inf}}$  for the reason stated above.

By substituting Eqs. (5), (20), (27) and (33) into Eq. (32), we are led to the following expression for the emission amplitude:

$$\mathcal{A}_{\omega l}^{\text{up/in}} = \frac{i q \sqrt{2l+1}}{4\pi \sqrt{\omega} A_{\omega l}^{\text{up/in}}} \int_{r_h}^{r_0} dr_s \frac{\Psi_{\omega l}^{\text{up/in}}(r_s) \exp(i\omega t_s)}{r_s \sqrt{E^2 - f(r_s)}}. \quad (34)$$

Using Eq. (26), we can rewrite Eq. (34) by integrating by parts as follows:

$$\mathcal{A}_{\omega l}^{\text{up/in}} = \frac{q \sqrt{2l+1}}{4\pi E \omega \sqrt{\omega} A_{\omega l}^{\text{up/in}}} \left[ -B + \int_{r_h}^{r_0} dr_s \left( \frac{\Psi_{\omega l}^{\text{up/in}}}{r_s} \frac{df}{dr_s} + \frac{f}{r_s} \frac{d\Psi_{\omega l}^{\text{up/in}}}{dr_s} - \frac{f \Psi_{\omega l}^{\text{up/in}}}{r_s^2} \right) \exp(i\omega t_s) \right], \quad (35)$$

where

$$B = \left[ \frac{f(r_s) \Psi_{\omega l}^{\text{up/in}}(r_s) \exp(i\omega t_s)}{r_s} \right]_{r_s=r_0}. \quad (36)$$

The expression (34), or equivalently (35), in fact represents the emission amplitude from a scalar source that suddenly appears at  $t_s = 0$  and starts falling. To obtain the amplitude from a scalar source that is static until  $t_s = 0$  and then starts

falling, we first convert the  $r_s$  integral in Eq. (34) for the amplitude back to the  $t_s$  integral using Eq. (26) and find

$$\begin{aligned} \mathcal{A}_{\omega l}^{\text{up/in}} &= \frac{iq\sqrt{2l+1}}{4\pi E\sqrt{\omega}A_{\omega l}^{\text{up/in}}} \int_{-\infty}^{\infty} dt_s \frac{f(r_s)}{r_s} \\ &\quad \times \Psi_{\omega l}^{\text{up/in}}(r_s) \exp(i\omega t_s). \end{aligned} \quad (37)$$

Since  $r_s(t_s) = r_0$  for  $t_s \leq 0$ , we can readily evaluate the integral over  $(-\infty, 0]$  by changing  $\exp(i\omega t_s)$  to  $\exp(i\omega t_s + \varepsilon t_s)$  with  $\varepsilon > 0$  and letting  $\varepsilon \rightarrow 0$ . We integrate by parts over  $[0, \infty)$  and find that the boundary term is canceled by the integral over  $(-\infty, 0]$ . Thus, the result turns out to be Eq. (35) with  $B = 0$ .

Finally, using Eq. (28), we write the emitted energy spectra as <sup>1</sup>:

$$E_{\omega l}^{\text{hor/inf}} = \omega |\mathcal{A}_{\omega l}^{\text{up/in}}|^2. \quad (38)$$

## 5 The Zero-frequency limit

In this section we obtain the zero-frequency limit (ZFL) of the spectra of the energy emitted to infinity [Eq. (28)], using approximate analytic solutions of Eq. (10), in order to check the results obtained for the energy spectra considering the full numerical solution.

Since there is only one parameter  $M$  with dimensions in Schwarzschild spacetime, the low-frequency limit is the limit where  $\omega \ll M^{-1}$ . Since the energy spectra  $E_{\omega l}^{\text{hor/inf}}$  are dimensionless, they are functions of  $M\omega$  for  $r_0 = \infty$ . Hence, their  $\omega \rightarrow 0$  limit for  $r_0 = \infty$  is achieved by letting  $M \rightarrow 0$  [45]. (Note that  $r_0$  introduces another parameter with dimensions if it is finite.) In this limit we may replace the potential  $V_l(r)$  in Eq. (11) by its leading term for large  $r$ ,

$$V_l(r) \approx l(l+1)/r^2, \quad (39)$$

and let

$$f(r) \approx 1. \quad (40)$$

Equation (10) in this approximation is the wave equation in Minkowski spacetime with the following familiar solutions:

$$(A_{\omega l}^{\text{in}})^{-1} \Psi_{\omega l}^{\text{in}}(r) \approx 2\omega r j_l(\omega r), \quad (41)$$

where  $j_l(\omega r)$  are the spherical Bessel functions [37], up to a phase factor. Thus, in the limit  $M \rightarrow 0$  Eq. (34) for  $r_0 = \infty$  becomes

$$\begin{aligned} \sqrt{\omega} \mathcal{A}_{\omega l}^{\text{in}} &= \frac{iq\sqrt{2l+1}}{2\pi} \sqrt{v_0^{-2} - 1} \\ &\quad \times \int_0^{\infty} \omega dr_s j_l(\omega r_s) \exp(-i\omega r_s/v_0) \\ &= \frac{q\sqrt{2l+1}}{2\pi} \sqrt{v_0^{-2} - 1} (-i)^l Q_l(v_0^{-1}), \end{aligned} \quad (42)$$

<sup>1</sup>Some authors define  $E_{\omega l}^{\text{hor/inf}}$  to be 1/2 times ours because the total energy emitted is obtained by integrating  $E^{\text{hor/inf}}$  over  $\omega$  from  $-\infty$  to  $\infty$  in their case.

where  $Q_l(z)$  is the Legendre function of the second kind with the branch cut  $[-1, 1]$ . Hence for  $r_0 = \infty$  we find the  $\omega \rightarrow 0$  limit of the spectra of the energy emitted to infinity,  $E_{\omega l}^{\text{inf}}$ , as

$$E_{0l}^{\text{inf}, r_0=\infty} = \frac{q^2(2l+1)}{4\pi^2} (v_0^{-2} - 1) [Q_l(v_0^{-1})]^2. \quad (43)$$

Now, if  $r$  is held fixed, then (see, e.g. Sec. VI of Ref. [32])

$$\lim_{\omega \rightarrow 0} (A_{\omega l}^{\text{in}})^{-1} \Psi_{\omega l}^{\text{in}}(r) = \delta_l^0 r. \quad (44)$$

For  $r_0$  finite this limit can be used for all  $r \leq r_0$  in Eq. (35) (with  $B = 0$ ). Thus, we find

$$\begin{aligned} E_{0l}^{\text{inf}} &= \frac{q^2 \delta_l^0}{4\pi^2 E^2} \left(1 - \frac{2M}{r_0}\right)^2 \\ &= \frac{q^2 \delta_l^0}{4\pi^2} \left(1 - \frac{2M}{r_0}\right) \text{ if } v_0 = 0. \end{aligned} \quad (45)$$

Note that this formula is not valid for  $r_0 = \infty$  because the limits  $\omega \rightarrow 0$  and  $r_0 \rightarrow \infty$  do not commute. The zero-frequency limit of  $(A_{\omega l}^{\text{up}})^{-1} \Psi_{\omega l}^{\text{up}}(r)$ , relevant to the radiation emitted to the horizon, is also known (see, e.g. Ref. [32]), and one can use them to find the zero-frequency limit of the spectra of energy emitted to the horizon,  $E_{\omega l}^{\text{hor}}$ , for finite  $r_0$  in a similar manner with the following result:

$$\begin{aligned} E_{0l}^{\text{hor}} &= \frac{(2l+1)q^2}{\pi^2 E^2} [Q_l(r_0/M - 1)]^2 \left(1 - \frac{2M}{r_0}\right)^2 \\ &= \frac{(2l+1)q^2}{\pi^2} [Q_l(r_0/M - 1)]^2 \left(1 - \frac{2M}{r_0}\right) \text{ if } v_0 = 0. \end{aligned} \quad (46)$$

## 6 Numerical results

In Sec. 4 we described how to find the energy spectra of massless scalar radiation from a source freely falling radially. In this section we present numerical evaluation of the energy spectra. As for the source's motion, we consider the following two distinct cases: (i) the source coming from  $r = \infty$  with non-vanishing initial velocity  $v_0$ , and (ii) the source released from rest at a certain position  $r = r_0$ .

The results for the spectra for the energy emitted to the horizon,  $E_{\omega l}^{\text{hor}}$ , and to infinity,  $E_{\omega l}^{\text{inf}}$ , for the radial infall of a source starting from  $r = \infty$  for selected values of initial velocity  $v_0$  are shown in Fig. 2. These results were obtained numerically from Eqs. (34) and (38), as a function of  $\omega$  and for selected values of the multipole number  $l$ . [We obtain the same results by using Eq. (35), instead of Eq. (34), and setting  $B = 0$ , because the boundary term (36) vanishes.] We note that the spectrum of energy emitted to the horizon,  $E_{\omega l}^{\text{hor}}$ , (plots on the left in Fig. 2) starts from zero (at  $\omega = 0$ ), reaches a maximum, and then slowly decreases to zero (for high values of  $\omega$ ). Note that the energy emitted

to the horizon does not decrease as the multipole number  $l$  increases unlike the energy emitted to infinity. This behavior of the spectra  $E_{\omega l}^{\text{hor}}$  is similar to that of the corresponding spectrum for the gravitational radiation [5]. It reflects the fact that the source has infinite self energy due to the Coulomb-like potential and that the region of large energy density passes through the horizon as the source approaches it. The spectrum of energy emitted to infinity,  $E_{\omega l}^{\text{inf}}$ , (plots on the right in Fig. 2) starts from a non-vanishing finite value (at  $\omega = 0$ ), and goes to zero for high frequencies. The contribution of higher multipoles decrease rapidly with increasing  $l$  as in the gravitational case [4]. These spectra were studied by Brito [45], and our results are in agreement with his. It is interesting that for high initial velocities the spectrum for each  $l \geq 1$  is approximately constant and drops to zero around the fundamental quasinormal frequency. [These frequencies  $\omega_{\text{qn}}$  are given as  $\omega_{\text{qn}} r_{\text{h}} = 0.215 (l = 0), 0.586 (l = 1), 0.967 (l = 2), 1.351 (l = 3)$  and  $1.733 (l = 4)$  (see, e.g. Ref. [46]).] The spectra for the gravitational and electromagnetic radiation behave in a similar manner [7, 13].

The results for the emitted energy spectra  $E_{\omega l}^{\text{hor}}$  and  $E_{\omega l}^{\text{inf}}$ , for the radial infall of a source starting from rest for selected values of position  $r_0$  obtained numerically from Eqs. (35) (with  $B = 0$ ) and (38), are shown in Fig. 3, as functions of  $\omega$  and for selected values of the multipole number  $l$ . We note that the emission to infinity is dominated by lower multipoles ( $l = 0, 1$ ) while there is substantial contribution from the modes with  $l \geq 2$  to the emission to the horizon, reflecting the region of high energy density surrounding the source passing through the horizon. Next we show the same spectra using Eq. (34) instead of Eq. (35) (with  $B = 0$ ). As we stated before, the emission in this case is from a source that emerges suddenly at  $r = r_0$  and starts falling. The results are shown in Fig. 4. We note that the spectra of the emitted energy both to the horizon and to infinity,  $E_{\omega l}^{\text{hor}}$  and  $E_{\omega l}^{\text{inf}}$ , vanish for both  $\omega = 0$  and  $\omega \rightarrow \infty$ , (i) oscillating between these limits, for mid-to-large values of  $r_0$  (e.g.,  $r_0 = 5 r_{\text{h}}$ ), or (ii) behaving with a Gaussian-like profile, for small values of  $r_0$  (e.g.,  $r_0 = 2.5 r_{\text{h}}$  and  $r_0 = 1.1 r_{\text{h}}$ ).

In the plots of Fig. 5, we show the energy emitted to infinity  $E_l^{\text{inf}}$ , obtained from Eq. (28), as a function of the initial velocity  $v_0$ . The monopole ( $l = 0$ ) emission is dominant for low initial velocities while higher multipoles ( $l \geq 1$ ) become significant for high initial velocities. We note that for  $l = 0$ , as the initial velocity  $v_0$  increases, the value of  $E_0^{\text{inf}}$  decreases. It is interesting that this behavior for the multipole number  $l = 0$  is the opposite to that for the multipole numbers  $l \geq 1$ . In the plots of Fig. 6, we show the emitted energy  $E_l^{\text{inf}}$ , obtained from Eq. (28), as a function of the position  $r_0$ . We note that as the position  $r_0$  gets closer to the BH event horizon, the emitted energy  $E_l^{\text{inf}}$  goes to zero as expected. The plot on the right uses Eq. (35) with  $B = 0$ . It can be seen that the emission is mainly with  $l = 0$  and  $l = 1$ , and

that it increases as a function of  $r_0$ . The plots on the left use Eq. (34). The spectrum does not decrease as a function of  $l$ . This is an ultraviolet effect arising from sudden emergence of a source at  $r = r_0$ .

In Tables 1, 2 and 3, we compare the zero-frequency limit (ZFL) of the energy spectra obtained numerically with the corresponding analytic results. In Table 1, we compare the ZFL of the spectrum of the energy radiated to infinity from a source infalling from  $r = \infty$  obtained analytically in Eq. (43), with the ones obtained using the numerical solution of Eq. (10) as a check of the numerical results. Similarly, in Table 2 we compare the ZFL for the spectrum of the energy radiated to infinity for the source infalling radially from rest from a certain position  $r_0$ , given by Eq. (45), with the ones obtained using the numerical solution of Eq. (10).

In Table 3 we compare the ZFL for the spectrum of the energy radiated to the event horizon for the source infalling radially from rest at a certain position  $r_0$ , given by Eq. (46), with the ones obtained using the numerical solution of Eq. (10). In all cases the ZFL of the numerical results agree very well with the analytic expressions.

**Table 1** Spectra of the energy radiated to infinity in the ZFL for multipole numbers  $l = 0, 1, 2$ , considering the source released from infinity with non-vanishing initial velocity. We compare the results obtained numerically by using Eq. (10) with the ones obtained analytically in Eq. (43).

$v_0$	Method	$l = 0$	$l = 1$	$l = 2$
0.5	Numerical	0.022854	0.002252	0.000176
	Analytic	0.022929	0.002216	0.000170
0.75	Numerical	0.018646	0.00524	0.001162
	Analytic	0.018650	0.00522	0.001150
0.95	Numerical	0.009132	0.007002	0.00406
	Analytic	0.009182	0.007072	0.00413

**Table 2** Spectra of the energy radiated to infinity in the ZFL for  $l = 0$ . The numerical results are compared with the exact values given by Eq. (45) (the results for  $l > 0$  are identically zero), considering the source released from rest at a certain finite position  $r_0$ .

$r_0/r_{\text{h}}$	Method	$l = 0$
1.1	Numerical	0.002312
	Analytic	0.002302
2.5	Numerical	0.015288
	Analytic	0.015198
5.0	Numerical	0.020384
	Analytic	0.020264

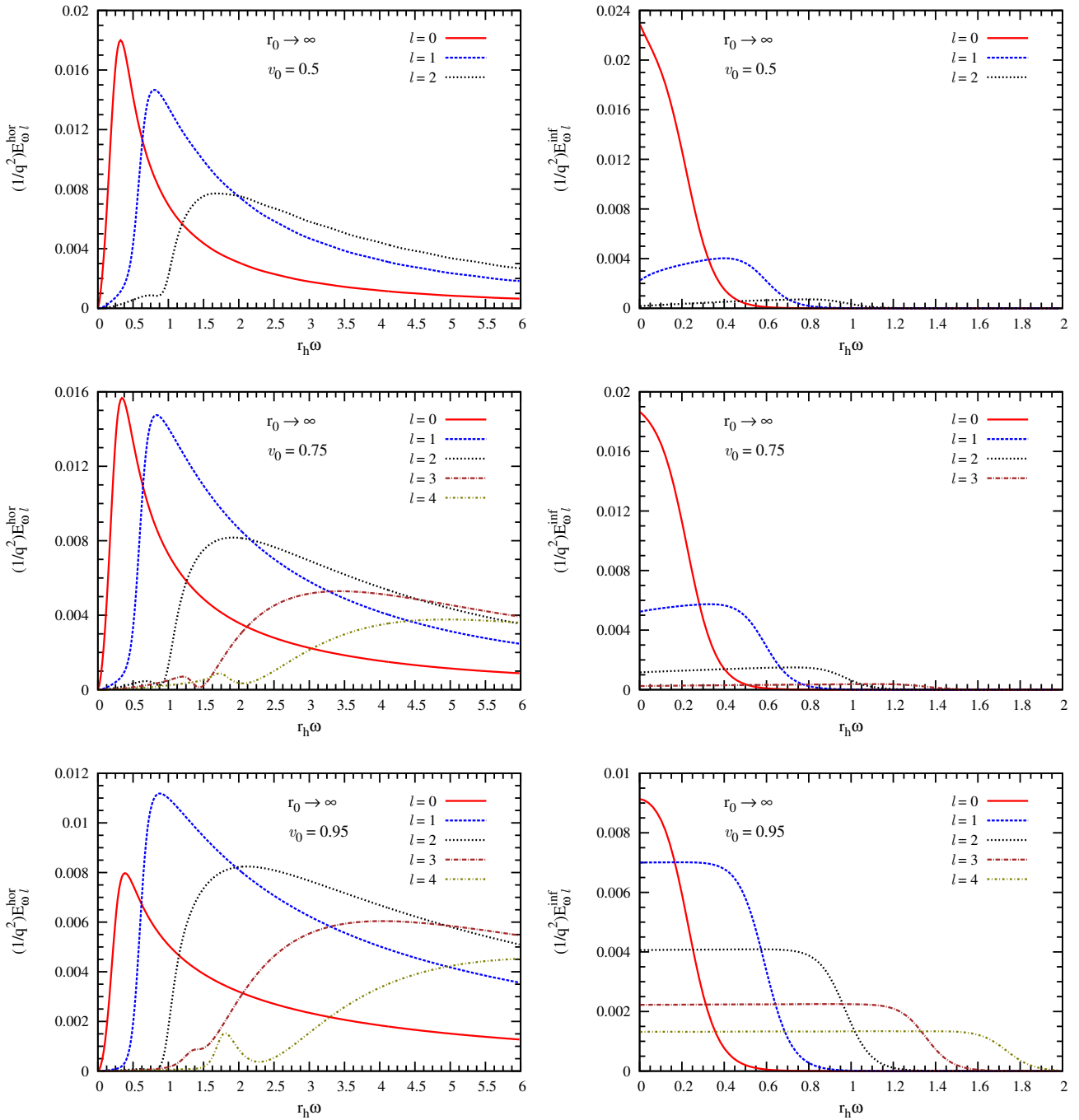


**Fig. 2** Numerical estimates of the spectra of the emitted energy,  $E_{\omega l}^{\text{hor}}$  (plots on the left) and  $E_{\omega l}^{\text{inf}}$  (plots on the right), as functions of  $\omega$ , for selected values of the multipole number, obtained from Eqs. (38) and (34), for the radial infall of a source from spatial infinity ( $r_0 \rightarrow \infty$ ), with the initial velocity  $v_0 = 0.5$  (plots at the top),  $v_0 = 0.75$  (plots in the middle) and  $v_0 = 0.95$  (plots at the bottom).

## 7 Summary

In this paper we studied, using the formalism of QFT at tree level, the radiation emission of massless scalar field from the radial infall of a source into a Schwarzschild BH. We computed numerically the spectra of the emitted energy,  $E_{\omega l}^{\text{hor}}$  (energy radiated to the event horizon) and  $E_{\omega l}^{\text{inf}}$  (energy ra-

diated to infinity), in two distinct situations related to the initial condition of the radial infall of a source, namely: (i) the source starting with non-vanishing velocity  $v_0$  from spatial infinity, and (ii) the source infalling from rest at a certain finite position  $r_0$ .

Let us summarize some aspects of the case in which the source comes from infinity with a certain non-vanishing ve-



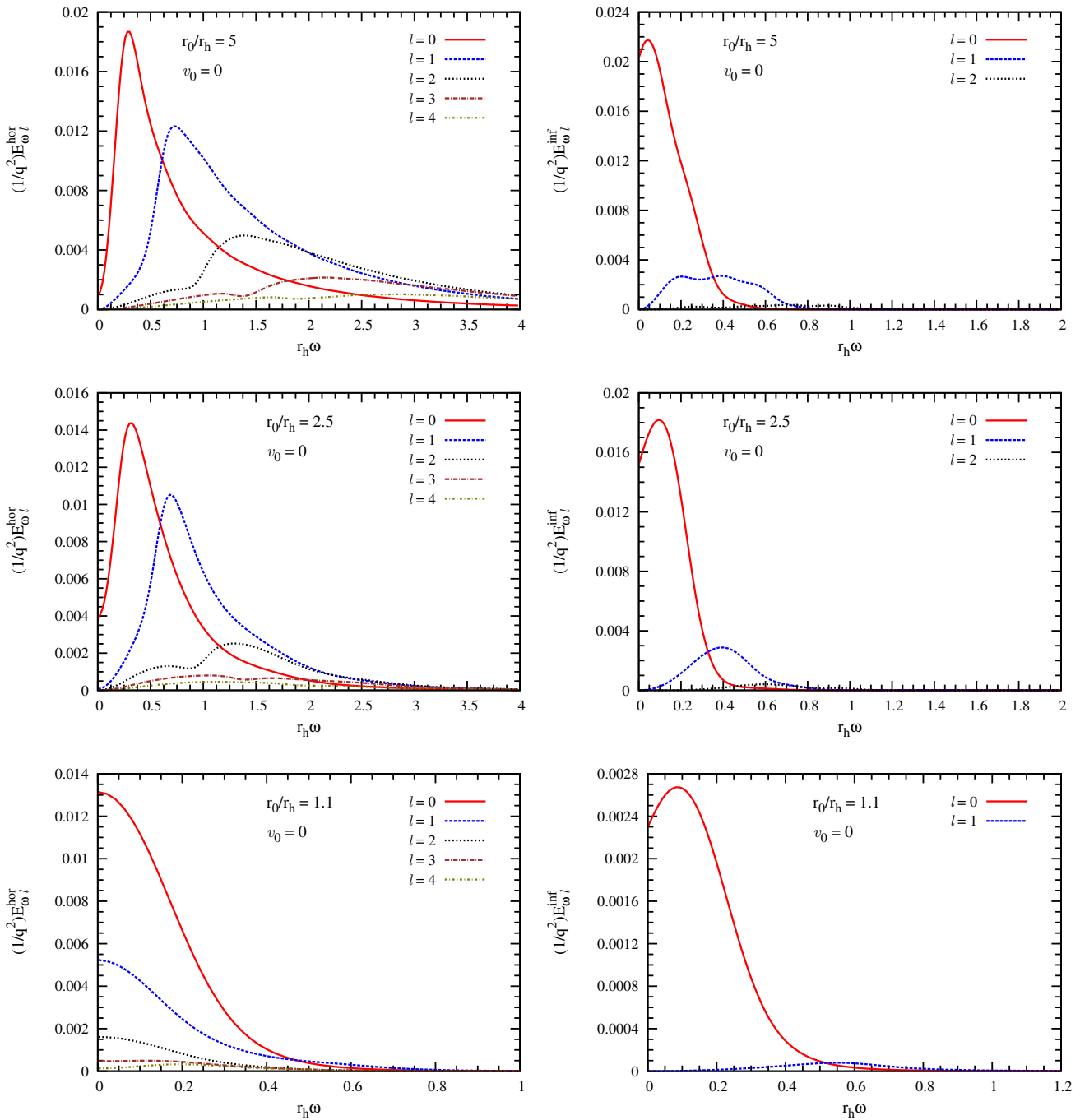


**Fig. 3** Numerical estimates of the spectra of the emitted energy,  $E_{\omega l}^{\text{hor}}$  (plots on the left) and  $E_{\omega l}^{\text{inf}}$  (plots on the right), as functions of  $\omega$ , for selected values of the multipole number, obtained from Eqs. (38) and (35) (with  $B = 0$ ), for a source infalling from rest ( $v_0 = 0$ ) at positions  $r_0 = 5 r_h$  (plots at the top),  $r_0 = 2.5 r_h$  (plots in the middle) and  $r_0 = 1.1 r_h$  (plots at the bottom).

locity  $v_0$ . For all multipole numbers  $l$  the spectra of the energy emitted to infinity are nonzero in the low-frequency limit. For high initial velocities the spectrum is approximately constant until the frequency is around the fundamental quasinormal frequency and then rapidly goes to zero. For low initial velocities the monopole ( $l = 0$ ) radiation and the dipole ( $l = 1$ ) (to a lesser extent) are dominant while higher

multipoles are significant at higher initial velocities. Interestingly, as the initial velocity  $v_0$  is increased, the emitted energy for the monopole radiation ( $l = 0$ ) decreases whereas that for the higher multipoles increases. The spectrum of the energy emitted to the event horizon starts from zero, increases to a maximum and decreases very slowly, reflecting the fact that, as the source falls toward the horizon, the

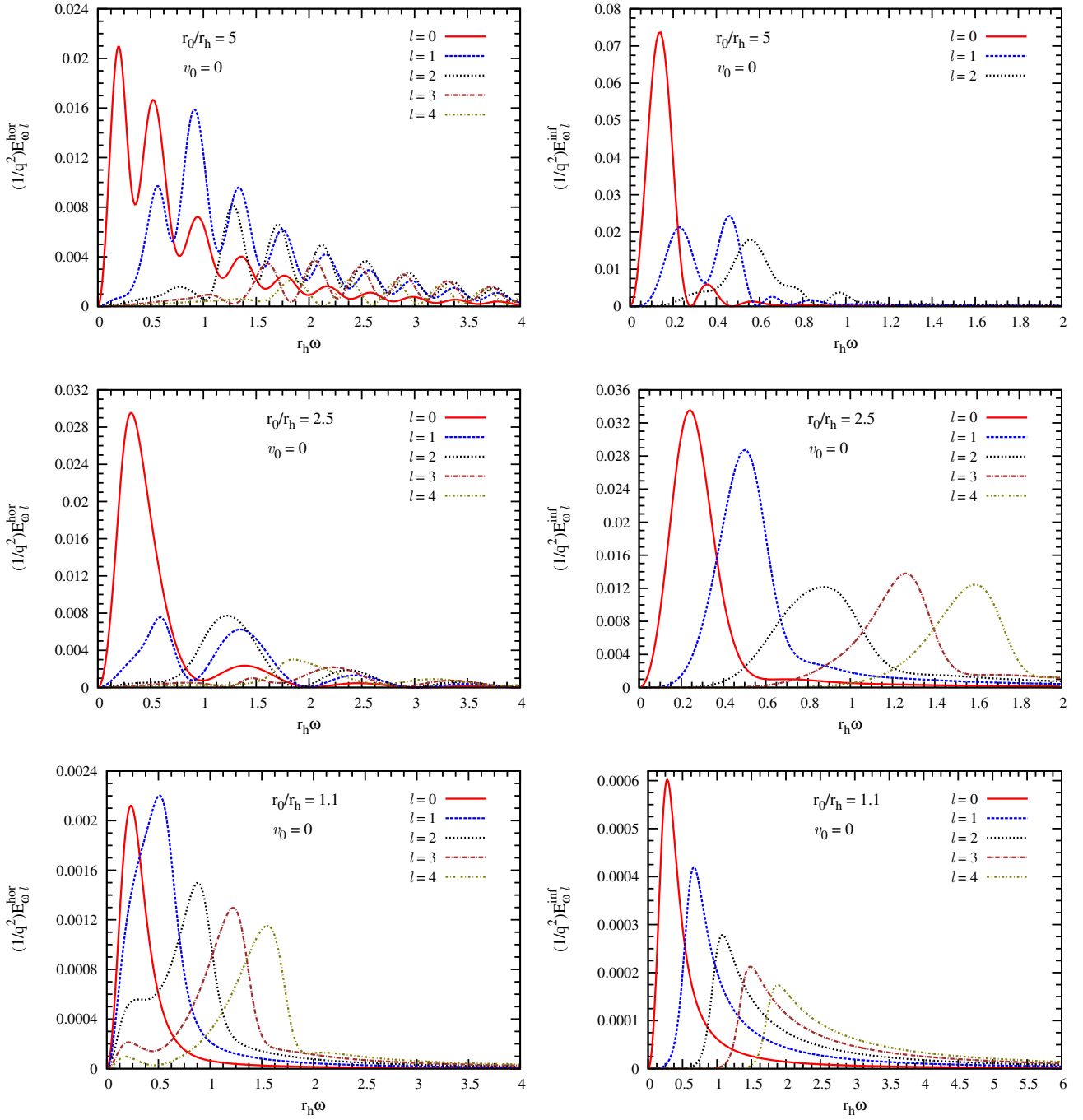


**Fig. 4** Numerical estimates of the spectra of the emitted energy,  $E_{\omega l}^{\text{hor}}$  (plots on the left) and  $E_{\omega l}^{\text{inf}}$  (plots on the right), as a function of  $\omega$ , for selected values of the multipole number, obtained from Eqs. (34) and (38), considering a source infalling from rest ( $v_0 = 0$ ) at positions  $r_0 = 5 r_h$  (plots at the top),  $r_0 = 2.5 r_h$  (plots in the middle) and  $r_0 = 1.1 r_h$  (plots at the bottom).

Coulomb-like energy of the source passes through the black hole.

Next, let us discuss some properties of the energy spectra for the case where the source starts falling from rest at a certain distance from the black hole. The monopole spectrum of the energy emitted to infinity starts from a nonzero value while, for  $l \geq 1$  the spectra start at zero. These spec-

tra all rise to a maximum and then decrease to zero. As for the spectrum of energy emitted to the event horizon, The emission is mainly with  $l = 0$  (monopole) and with  $l = 1$  (dipole). The emission to the horizon has more contribution from higher multipoles. We also pointed out that a naïve calculation would lead to a source appearing abruptly and then starting to fall and that a boundary term needs to be sub-

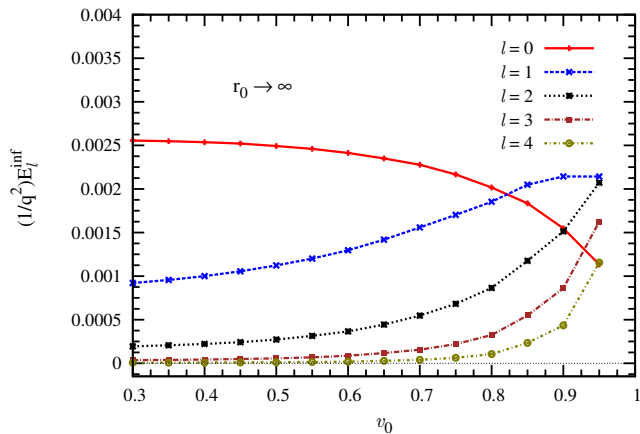


**Fig. 5** Numerical estimates of the emitted energy radiated to infinity,  $E_l^{\text{inf}}$ , as a function of  $v_0$ , for multipole numbers  $l = 0, 1, 2, 3, 4$ , obtained from Eq. (28).

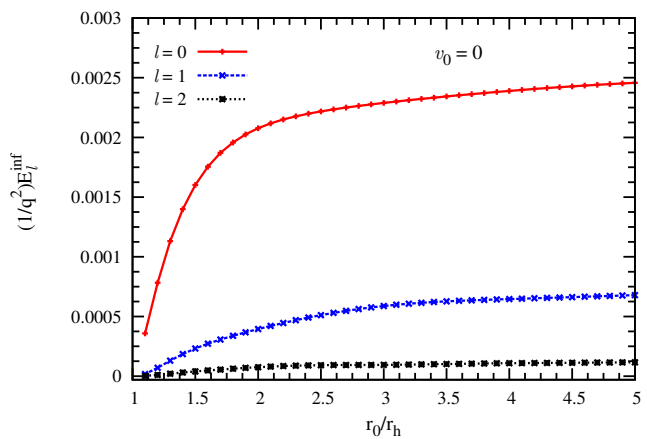
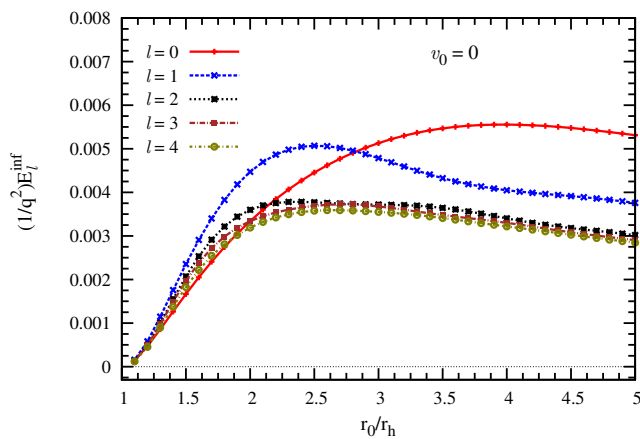


**Fig. 6** Numerical estimates of the emitted energy radiated to infinity,  $E_l^{\text{inf}}$ , as a function of  $r_0$ , obtained using Eq. (28), considering Eq. (34) (plots on the left) and Eq. (35) with  $B = 0$  (plots on the right), for selected choices of multipole numbers obtained from Eq. (28).

**Table 3** Spectra of energy radiated to the event horizon in the ZFL. The numerical results are compared with the exact values given by Eq. (46), for  $l = 0, 1, 2$ , considering the source released from rest at a certain finite position  $r_0$ .

$r_0/r_h$	Method	$l = 0$	$l = 1$	$l = 2$
1.1	Numerical	0.013133	0.005228	0.001612
	Analytic	0.013240	0.005319	0.001667
2.5	Numerical	0.003944	0.000081	$< 10^{-6}$
	Analytic	0.003965	0.000085	$< 10^{-6}$
5.0	Numerical	0.001000	$< 10^{-6}$	$< 10^{-8}$
	Analytic	0.001009	$< 10^{-6}$	$< 10^{-8}$

tracted in order to calculate the emission from a source at rest and then starting to fall.

Finally, we note that the behavior of the spectra of the emitted energy,  $E_{\omega l}^{\text{inf}}$ , and the total emitted energy  $E_l^{\text{inf}}$ , to infinity for multipole numbers  $l \geq 1$  are similar to the elec-

tromagnetic and gravitational cases (see, e.g, Refs. [7, 8, 10, 13]).

## Acknowledgments

The authors acknowledge Conselho Nacional de Desenvolvimento Científico e Tecnológico (CNPq) and Coordenação de Aperfeiçoamento de Pessoal de Nível Superior (CAPES) for partial financial support. AH also acknowledges partial support from the Abdus Salam International Centre for Theoretical Physics through Visiting Scholar/Consultant Programme. AH thanks the Universidade Federal do Pará in Belém for kind hospitality. LO is grateful to University of York for kind hospitality.

## References

1. C. W. Misner, K. S. Thorne, and J. A. Wheeler, *Gravitation* (W. H. Freeman and Co., New York, 1973).
2. J. Mathews, Gravitational Multipole Radiation, *J. Soc. Ind. Appl. Math.* **10**, 768 (1962).
3. F. J. Zerilli, Gravitational field of a particle falling in a Schwarzschild geometry analyzed in tensor harmonics, *Phys. Rev. D* **2**, 2141 (1970).
4. M. Davis, R. Ruffini, W. H. Press and R. H. Price, Gravitational radiation from a particle falling radially into a Schwarzschild black hole, *Phys. Rev. Lett.* **27**, 1466 (1971).
5. M. Davis, R. Ruffini and J. Tiomno, Pulses of gravitational radiation of a particle falling radially into a Schwarzschild black hole, *Phys. Rev. D* **5**, 2932 (1972).
6. T. Regge and J. A. Wheeler, Stability of a Schwarzschild singularity, *Phys. Rev.* **108**, 1063 (1957).
7. R. Ruffini, Gravitational radiation from a mass projected into a Schwarzschild black hole, *Phys. Rev. D* **7**, 972 (1973).
8. C. O. Lousto and R. H. Price, Head-on collisions of black holes: The particle limit, *Phys. Rev. D* **55**, 2124 (1997) [gr-qc/9609012].
9. K. Martel and E. Poisson, One parameter family of time symmetric initial data for the radial infall of a particle into a Schwarzschild black hole, *Phys. Rev. D* **66**, 084001 (2002) [gr-qc/0107104].
10. V. Cardoso and J. P. S. Lemos, Gravitational radiation from collisions at the speed of light: A massless particle falling into a Schwarzschild black hole, *Phys. Lett. B* **538**, 1 (2002) [gr-qc/0202019].
11. V. Cardoso and J. P. S. Lemos, The radial infall of a highly relativistic point particle into a Kerr black hole along the symmetry axis, *Gen. Rel. Grav.* **35**, 327 (2003) [gr-qc/0207009].
12. V. Cardoso and J. P. S. Lemos, Gravitational radiation from the radial infall of highly relativistic point particles into Kerr black holes, *Phys. Rev. D* **67**, 084005 (2003) [gr-qc/0211094].
13. V. Cardoso, J. P. S. Lemos and S. Yoshida, Electromagnetic radiation from collisions at almost the speed of light: An extremely relativistic charged particle falling into a Schwarzschild black hole, *Phys. Rev. D* **68**, 084011 (2003) [gr-qc/0307104].
14. E. Berti, V. Cardoso and C. M. Will, Considerations on the excitation of black hole quasinormal modes, *AIP Conf. Proc.* **848**, 687 (2006) [gr-qc/0601077].
15. E. Berti, V. Cardoso, T. Hinderer, M. Lemos, F. Pretorius, U. Sperhake and N. Yunes, Semianalytical estimates of scattering thresholds and gravitational radiation in ultrarelativistic black hole encounters, *Phys. Rev. D* **81**, 104048 (2010) [arXiv:1003.0812 [gr-qc]].
16. E. Berti, V. Cardoso and B. Kipapa, Up to eleven: radiation from particles with arbitrary energy falling into higher-dimensional black holes, *Phys. Rev. D* **83**, 084018 (2011) [arXiv:1010.3874 [gr-qc]].
17. E. Mitsou, Gravitational radiation from radial infall of a particle into a Schwarzschild black hole. A numerical study of the spectra, quasi-normal modes and power-law tails, *Phys. Rev. D* **83**, 044039 (2011) [arXiv:1012.2028 [gr-qc]].
18. L. C. B. Crispino, G. E. A. Matsas and A. Higuchi, Scalar radiation emitted from a source rotating around a black hole, *Class. Quant. Grav.* **17**, 19 (2000).
19. L. C. B. Crispino, A. Higuchi and G. E. A. Matsas, Corrigendum: Scalar radiation emitted from a source rotating around a black hole (2000 *Class. Quantum Grav.* **17** 19), *Class. Quant. Grav.* **33**, 209502 (2016).
20. J. Castiñeiras, L. C. B. Crispino, R. Murta and G. E. A. Matsas, Semiclassical approach to black hole absorption of electromagnetic radiation emitted by a rotating charge, *Phys. Rev. D* **71**, 104013 (2005) [gr-qc/0503050].
21. J. Castiñeiras, L. C. B. Crispino and D. P. M. Filho, Source coupled to the massive scalar field orbiting a stellar object, *Phys. Rev. D* **75**, 024012 (2007).
22. L. C. B. Crispino, Synchrotron scalar radiation from a source in ultrarelativistic circular orbits around a Schwarzschild black hole, *Phys. Rev. D* **77**, 047503 (2008).
23. L. C. B. Crispino, A. R. R. da Silva and G. E. A. Matsas, Scalar radiation emitted from a rotating source around a Reissner-Nordstrom black hole, *Phys. Rev. D* **79**, 024004 (2009) [arXiv:0806.1537 [gr-qc]].
24. L. C. B. Crispino, J. L. C. da Cruz Filho and P. S. Letelier, Pseudo-Newtonian potentials and the radiation emitted by a source swirling around a stellar object, *Phys. Lett. B* **697**, 506 (2011).
25. C. F. B. Macedo, L. C. B. Crispino and V. Cardoso, Semiclassical analysis of the scalar geodesic synchrotron radiation in Kerr spacetime, *Phys. Rev. D* **86**, 024002 (2012).
26. D. T. Alves and L. C. B. Crispino, Response rate of a uniformly accelerated source in the presence of boundaries, *Phys. Rev. D* **70**, 107703 (2004).
27. D. T. Alves, L. C. B. Crispino, M. C. de Lima and A. Higuchi, Influence of boundary conditions on the radiation emitted by an accelerated source, *Phys. Rev. D* **81**, 065002 (2010).
28. J. Castiñeiras, E. B. S. Correa, L. C. B. Crispino and G. E. A. Matsas, Quantization of the Proca field in the Rindler wedge and the interaction of uniformly accelerated currents with massive vector bosons from the Unruh thermal bath, *Phys. Rev. D* **84**, 025010 (2011)

- [arXiv:1108.2813 [gr-qc]].
29. J. Castiñeiras, L. C. B. Crispino, G. E. A. Matsas and D. A. T. Vanzella, Free massive particles with total energy  $E$  less than  $mc^2$  in curved space-times, *Phys. Rev. D* **65**, 104019 (2002) [gr-qc/0201093].
  30. L. C. B. Crispino, A. Higuchi and G. E. A. Matsas, Is the equivalence for the response of static scalar sources in the Schwarzschild and Rindler spacetimes valid only in four dimensions?, *Phys. Rev. D* **70**, 127504 (2004) [gr-qc/0410139].
  31. A. Higuchi, G. E. A. Matsas and D. Sudarsky, Do static sources outside a Schwarzschild black hole radiate?, *Phys. Rev. D* **56**, 6071 (1997) [gr-qc/9609025].
  32. A. Higuchi, G. E. A. Matsas and D. Sudarsky, Interaction of Hawking radiation with static sources outside a Schwarzschild black hole, *Phys. Rev. D* **58**, 104021 (1998) [gr-qc/9806093].
  33. L. C. B. Crispino, A. Higuchi and G. E. A. Matsas, Interaction of Hawking radiation and a static electric charge, *Phys. Rev. D* **58**, 084027 (1998) [gr-qc/9804066].
  34. L. C. B. Crispino, A. Higuchi and G. E. A. Matsas, Quantization of the electromagnetic field outside static black holes and its application to low-energy phenomena, *Phys. Rev. D* **63**, 124008 (2001) [Erratum-ibid. *D* **80**, 029906 (2009)] [gr-qc/0011070].
  35. D. N. Page, Particle Emission Rates from a Black Hole: Massless Particles from an Uncharged, Nonrotating Hole, *Phys. Rev. D* **13**, 198 (1976).
  36. N. D. Birrel and P. C. W. Davies, *Quantum fields in curved space* (Cambridge University Press, New York 1982).
  37. G. B. Arfken and H. J. Webber, *Mathematical Methods for Physicists* (Elsevier Academic Press, San Diego, 2005).
  38. R. Wald, *General Relativity* (The University of Chicago Press, Chicago, 1984).
  39. M. P. Hobson, G. Efstathiou and A. N. Lasenby, *General Relativity – An Introduction for Physicists* (Cambridge University Press, Cambridge, 2006).
  40. D. G. Boulware, Quantum field theory in Schwarzschild and Rindler spaces, *Phys. Rev. D* **11**, 1404 (1975).
  41. W. G. Unruh, Note on black hole evaporation, *Phys. Rev. D* **14**, 870 (1976).
  42. J. B. Hartle and S. W. Hawking, Path integral derivation of black hole radiance, *Phys. Rev. D* **13**, 2188 (1976).
  43. R. P. Bernar, L. C. B. Crispino and A. Higuchi, Gravitational waves emitted by a particle rotating around a Schwarzschild black hole: A semiclassical approach, *Phys. Rev. D* **95**, 064042 (2017) [arXiv:1703.10648 [gr-qc]].
  44. D. W. Sciama, P. Candelas and D. Deutsch, Quantum field theory, horizons and thermodynamics, *Adv. Phys.* **30**, 327 (1981).
  45. R. Brito, Dynamics around black holes: Radiation emission and tidal effects, arXiv:1211.1679 [gr-qc].
  46. E. Abdalla and D. Giugno, An extensive search for overtones in Schwarzschild black hole, *Braz. J. Phys.* **37**, 450 (2007).